

Evidence for the Rare Decay $B \rightarrow J/\psi\eta\mathbf{K}$

The *BABAR* Collaboration

July 15, 2003

Abstract

We report evidence for the B meson decays, $B^\pm \rightarrow J/\psi\eta K^\pm$ and $B^0 \rightarrow J/\psi\eta K_S^0$, using 90 million $B\bar{B}$ events collected at the $\Upsilon(4S)$ resonance with the *BABAR* detector at the PEP-II e^+e^- asymmetric-energy storage ring. We obtain preliminary branching fractions in the charged and neutral channels of $(10.8 \pm 2.3(stat.) \pm 2.4(syst.)) \times 10^{-5}$ and $(8.4 \pm 2.6(stat.) \pm 2.7(syst.)) \times 10^{-5}$, respectively.

Presented at the International Europhysics Conference On High-Energy Physics (HEP 2003),
7/17—7/23/2003, Aachen, Germany

Stanford Linear Accelerator Center, Stanford University, Stanford, CA 94309

Work supported in part by Department of Energy contract DE-AC03-76SF00515.

The BABAR Collaboration,

B. Aubert, R. Barate, D. Boutigny, J.-M. Gaillard, A. Hicheur, Y. Karyotakis, J. P. Lees, P. Robbe,
V. Tisserand, A. Zghiche

Laboratoire de Physique des Particules, F-74941 Annecy-le-Vieux, France

A. Palano, A. Pompili

Università di Bari, Dipartimento di Fisica and INFN, I-70126 Bari, Italy

J. C. Chen, N. D. Qi, G. Rong, P. Wang, Y. S. Zhu

Institute of High Energy Physics, Beijing 100039, China

G. Eigen, I. Ofte, B. Stugu

University of Bergen, Inst. of Physics, N-5007 Bergen, Norway

G. S. Abrams, A. W. Borgland, A. B. Breon, D. N. Brown, J. Button-Shafer, R. N. Cahn, E. Charles,
C. T. Day, M. S. Gill, A. V. Gritsan, Y. Groysman, R. G. Jacobsen, R. W. Kadel, J. Kadyk, L. T. Kerth,
Yu. G. Kolomensky, J. F. Kral, G. Kukartsev, C. LeClerc, M. E. Levi, G. Lynch, L. M. Mir, P. J. Oddone,
T. J. Orimoto, M. Pripstein, N. A. Roe, A. Romosan, M. T. Ronan, V. G. Shelkov, A. V. Telnov,
W. A. Wenzel

Lawrence Berkeley National Laboratory and University of California, Berkeley, CA 94720, USA

K. Ford, T. J. Harrison, C. M. Hawkes, D. J. Knowles, S. E. Morgan, R. C. Penny, A. T. Watson,
N. K. Watson

University of Birmingham, Birmingham, B15 2TT, United Kingdom

T. Deppermann, K. Goetzen, H. Koch, B. Lewandowski, M. Pelizaeus, K. Peters, H. Schmuecker,
M. Steinke

Ruhr Universität Bochum, Institut für Experimentalphysik 1, D-44780 Bochum, Germany

N. R. Barlow, J. T. Boyd, N. Chevalier, W. N. Cottingham, M. P. Kelly, T. E. Latham, C. Mackay,
F. F. Wilson

University of Bristol, Bristol BS8 1TL, United Kingdom

K. Abe, T. Cuhadar-Donszelmann, C. Hearty, T. S. Mattison, J. A. McKenna, D. Thiessen

University of British Columbia, Vancouver, BC, Canada V6T 1Z1

P. Kyberd, A. K. McKemey

Brunel University, Uxbridge, Middlesex UB8 3PH, United Kingdom

V. E. Blinov, A. D. Bukin, V. B. Golubev, V. N. Ivanchenko, E. A. Kravchenko, A. P. Onuchin,
S. I. Serednyakov, Yu. I. Skovpen, E. P. Solodov, A. N. Yushkov

Budker Institute of Nuclear Physics, Novosibirsk 630090, Russia

D. Best, M. Bruinsma, M. Chao, D. Kirkby, A. J. Lankford, M. Mandelkern, R. K. Mommsen, W. Roethel,
D. P. Stoker

University of California at Irvine, Irvine, CA 92697, USA

C. Buchanan, B. L. Hartfiel

University of California at Los Angeles, Los Angeles, CA 90024, USA

B. C. Shen

University of California at Riverside, Riverside, CA 92521, USA

D. del Re, H. K. Hadavand, E. J. Hill, D. B. MacFarlane, H. P. Paar, Sh. Rahatlou, U. Schwanke,
V. Sharma

University of California at San Diego, La Jolla, CA 92093, USA

J. W. Berryhill, C. Campagnari, B. Dahmes, N. Kuznetsova, S. L. Levy, O. Long, A. Lu, M. A. Mazur,
J. D. Richman, W. Verkerke

University of California at Santa Barbara, Santa Barbara, CA 93106, USA

T. W. Beck, J. Beringer, A. M. Eisner, C. A. Heusch, W. S. Lockman, T. Schalk, R. E. Schmitz,
B. A. Schumm, A. Seiden, M. Turri, W. Walkowiak, D. C. Williams, M. G. Wilson

University of California at Santa Cruz, Institute for Particle Physics, Santa Cruz, CA 95064, USA

J. Albert, E. Chen, G. P. Dubois-Felsmann, A. Dvoretzkii, D. G. Hitlin, I. Narsky, F. C. Porter, A. Ryd,
A. Samuel, S. Yang

California Institute of Technology, Pasadena, CA 91125, USA

S. Jayatileke, G. Mancinelli, B. T. Meadows, M. D. Sokoloff

University of Cincinnati, Cincinnati, OH 45221, USA

T. Abe, F. Blanc, P. Bloom, S. Chen, P. J. Clark, W. T. Ford, U. Nauenberg, A. Olivas, P. Rankin, J. Roy,
J. G. Smith, W. C. van Hoek, L. Zhang

University of Colorado, Boulder, CO 80309, USA

J. L. Harton, T. Hu, A. Soffer, W. H. Toki, R. J. Wilson, J. Zhang

Colorado State University, Fort Collins, CO 80523, USA

D. Altenburg, T. Brandt, J. Brose, T. Colberg, M. Dickopp, R. S. Dubitzky, A. Hauke, H. M. Lacker,
E. Maly, R. Müller-Pfefferkorn, R. Nogowski, S. Otto, J. Schubert, K. R. Schubert, R. Schwierz, B. Spaan,
L. Wilden

Technische Universität Dresden, Institut für Kern- und Teilchenphysik, D-01062 Dresden, Germany

D. Bernard, G. R. Bonneaud, F. Brochard, J. Cohen-Tanugi, P. Grenier, Ch. Thiebaux, G. Vasileiadis,
M. Verderi

Ecole Polytechnique, LLR, F-91128 Palaiseau, France

A. Khan, D. Lavin, F. Muheim, S. Playfer, J. E. Swain, J. Tinslay

University of Edinburgh, Edinburgh EH9 3JZ, United Kingdom

M. Andreotti, V. Azzolini, D. Bettoni, C. Bozzi, R. Calabrese, G. Cibinetto, E. Luppi, M. Negrini,
L. Piemontese, A. Sarti

Università di Ferrara, Dipartimento di Fisica and INFN, I-44100 Ferrara, Italy

E. Treadwell

Florida A&M University, Tallahassee, FL 32307, USA

F. Anulli,¹ R. Baldini-Ferroli, M. Biasini,¹ A. Calcaterra, R. de Sangro, D. Falciari, G. Finocchiaro,
P. Patteri, I. M. Peruzzi,¹ M. Piccolo, M. Pioppi,¹ A. Zallo

Laboratori Nazionali di Frascati dell'INFN, I-00044 Frascati, Italy

A. Buzzo, R. Capra, R. Contri, G. Crosetti, M. Lo Vetere, M. Macri, M. R. Monge, S. Passaggio,
C. Patrignani, E. Robutti, A. Santroni, S. Tosi

Università di Genova, Dipartimento di Fisica and INFN, I-16146 Genova, Italy

S. Bailey, M. Morii, E. Won

Harvard University, Cambridge, MA 02138, USA

W. Bhimji, D. A. Bowerman, P. D. Dauncey, U. Egede, I. Eschrich, J. R. Gaillard, G. W. Morton,
J. A. Nash, P. Sanders, G. P. Taylor

Imperial College London, London, SW7 2BW, United Kingdom

G. J. Grenier, S.-J. Lee, U. Mallik

University of Iowa, Iowa City, IA 52242, USA

J. Cochran, H. B. Crawley, J. Lamsa, W. T. Meyer, S. Prell, E. I. Rosenberg, J. Yi

Iowa State University, Ames, IA 50011-3160, USA

M. Davier, G. Grosdidier, A. Höcker, S. Laplace, F. Le Diberder, V. Lepeltier, A. M. Lutz, T. C. Petersen,
S. Plaszczynski, M. H. Schune, L. Tantot, G. Wormser

Laboratoire de l'Accélérateur Linéaire, F-91898 Orsay, France

V. Brigljević, C. H. Cheng, D. J. Lange, D. M. Wright

Lawrence Livermore National Laboratory, Livermore, CA 94550, USA

A. J. Bevan, J. P. Coleman, J. R. Fry, E. Gabathuler, R. Gamet, M. Kay, R. J. Parry, D. J. Payne,
R. J. Sloane, C. Touramanis

University of Liverpool, Liverpool L69 3BX, United Kingdom

J. J. Back, P. F. Harrison, H. W. Shorthouse, P. Strother, P. B. Vidal

Queen Mary, University of London, E1 4NS, United Kingdom

C. L. Brown, G. Cowan, R. L. Flack, H. U. Flaecher, S. George, M. G. Green, A. Kurup, C. E. Marker,
T. R. McMahon, S. Ricciardi, F. Salvatore, G. Vaitsas, M. A. Winter

University of London, Royal Holloway and Bedford New College, Egham, Surrey TW20 0EX, United Kingdom

D. Brown, C. L. Davis

University of Louisville, Louisville, KY 40292, USA

J. Allison, R. J. Barlow, A. C. Forti, P. A. Hart, F. Jackson, G. D. Lafferty, A. J. Lyon, J. H. Weatherall,
J. C. Williams

University of Manchester, Manchester M13 9PL, United Kingdom

A. Farbin, A. Jawahery, D. Kovalskyi, C. K. Lae, V. Lillard, D. A. Roberts

University of Maryland, College Park, MD 20742, USA

¹Also with Università di Perugia, Perugia, Italy

G. Blaylock, C. Dallapiccola, K. T. Flood, S. S. Hertzbach, R. Kofler, V. B. Koptchev, T. B. Moore,
S. Saremi, H. Staengle, S. Willocq

University of Massachusetts, Amherst, MA 01003, USA

R. Cowan, G. Sciolla, F. Taylor, R. K. Yamamoto

Massachusetts Institute of Technology, Laboratory for Nuclear Science, Cambridge, MA 02139, USA

D. J. J. Mangeol, M. Milek, P. M. Patel

McGill University, Montréal, QC, Canada H3A 2T8

A. Lazzaro, F. Palombo

Università di Milano, Dipartimento di Fisica and INFN, I-20133 Milano, Italy

J. M. Bauer, L. Cremaldi, V. Eschenburg, R. Godang, R. Kroeger, J. Reidy, D. A. Sanders, D. J. Summers,
H. W. Zhao

University of Mississippi, University, MS 38677, USA

S. Brunet, D. Cote-Ahern, C. Hast, P. Taras

Université de Montréal, Laboratoire René J. A. Lévesque, Montréal, QC, Canada H3C 3J7

H. Nicholson

Mount Holyoke College, South Hadley, MA 01075, USA

C. Cartaro, N. Cavallo,² G. De Nardo, F. Fabozzi,² C. Gatto, L. Lista, P. Paolucci, D. Piccolo, C. Sciacca
Università di Napoli Federico II, Dipartimento di Scienze Fisiche and INFN, I-80126, Napoli, Italy

M. A. Baak, G. Raven

NIKHEF, National Institute for Nuclear Physics and High Energy Physics, NL-1009 DB Amsterdam, The Netherlands

J. M. LoSecco

University of Notre Dame, Notre Dame, IN 46556, USA

T. A. Gabriel

Oak Ridge National Laboratory, Oak Ridge, TN 37831, USA

B. Brau, K. K. Gan, K. Honscheid, D. Hufnagel, H. Kagan, R. Kass, T. Pulliam, Q. K. Wong

Ohio State University, Columbus, OH 43210, USA

J. Brau, R. Frey, C. T. Potter, N. B. Sinev, D. Strom, E. Torrence

University of Oregon, Eugene, OR 97403, USA

F. Colecchia, A. Dorigo, F. Galeazzi, M. Margoni, M. Morandin, M. Posocco, M. Rotondo, F. Simonetto,
R. Stroili, G. Tiozzo, C. Voci

Università di Padova, Dipartimento di Fisica and INFN, I-35131 Padova, Italy

M. Benayoun, H. Briand, J. Chauveau, P. David, Ch. de la Vaissière, L. Del Buono, O. Hamon,
M. J. J. John, Ph. Leruste, J. Ocariz, M. Pivk, L. Roos, J. Stark, S. T'Jampens, G. Therin

Universités Paris VI et VII, Lab de Physique Nucléaire H. E., F-75252 Paris, France

²Also with Università della Basilicata, Potenza, Italy

P. F. Manfredi, V. Re

Università di Pavia, Dipartimento di Elettronica and INFN, I-27100 Pavia, Italy

P. K. Behera, L. Gladney, Q. H. Guo, J. Panetta

University of Pennsylvania, Philadelphia, PA 19104, USA

C. Angelini, G. Batignani, S. Bettarini, M. Bondioli, F. Bucci, G. Calderini, M. Carpinelli, F. Forti,
M. A. Giorgi, A. Lusiani, G. Marchiori, F. Martinez-Vidal,³ M. Morganti, N. Neri, E. Paoloni, M. Rama,
G. Rizzo, F. Sandrelli, J. Walsh

Università di Pisa, Dipartimento di Fisica, Scuola Normale Superiore and INFN, I-56127 Pisa, Italy

M. Haire, D. Judd, K. Paick, D. E. Wagoner

Prairie View A&M University, Prairie View, TX 77446, USA

N. Danielson, P. Elmer, C. Lu, V. Miftakov, J. Olsen, A. J. S. Smith, H. A. Tanaka, E. W. Varnes

Princeton University, Princeton, NJ 08544, USA

F. Bellini, G. Cavoto,⁴ R. Faccini,⁵ F. Ferrarotto, F. Ferroni, M. Gaspero, M. A. Mazzoni, S. Morganti,
M. Pierini, G. Piredda, F. Safai Tehrani, C. Voena

Università di Roma La Sapienza, Dipartimento di Fisica and INFN, I-00185 Roma, Italy

S. Christ, G. Wagner, R. Waldi

Universität Rostock, D-18051 Rostock, Germany

T. Adye, N. De Groot, B. Franek, N. I. Geddes, G. P. Gopal, E. O. Olaiya, S. M. Xella

Rutherford Appleton Laboratory, Chilton, Didcot, Oxon, OX11 0QX, United Kingdom

R. Aleksan, S. Emery, A. Gaidot, S. F. Ganzhur, P.-F. Giraud, G. Hamel de Monchenault, W. Kozanecki,
M. Langer, M. Legendre, G. W. London, B. Mayer, G. Schott, G. Vasseur, Ch. Yeche, M. Zito

DSM/Daphnia, CEA/Saclay, F-91191 Gif-sur-Yvette, France

M. V. Purohit, A. W. Weidemann, F. X. Yumiceva

University of South Carolina, Columbia, SC 29208, USA

D. Aston, R. Bartoldus, N. Berger, A. M. Boyarski, O. L. Buchmueller, M. R. Convery, D. P. Coupal,
D. Dong, J. Dorfan, D. Dujmic, W. Dunwoodie, R. C. Field, T. Glanzman, S. J. Gowdy, E. Grauges-Pous,
T. Hadig, V. Halyo, T. Hryn'ova, W. R. Innes, C. P. Jessop, M. H. Kelsey, P. Kim, M. L. Kocian,
U. Langenegger, D. W. G. S. Leith, S. Luitz, V. Luth, H. L. Lynch, H. Marsiske, R. Messner, D. R. Muller,
C. P. O'Grady, V. E. Ozcan, A. Perazzo, M. Perl, S. Petrak, B. N. Ratcliff, S. H. Robertson, A. Roodman,
A. A. Salnikov, R. H. Schindler, J. Schwiening, G. Simi, A. Snyder, A. Soha, J. Stelzer, D. Su,
M. K. Sullivan, J. Va'vra, S. R. Wagner, M. Weaver, A. J. R. Weinstein, W. J. Wisniewski, D. H. Wright,
C. C. Young

Stanford Linear Accelerator Center, Stanford, CA 94309, USA

P. R. Burchat, A. J. Edwards, T. I. Meyer, B. A. Petersen, C. Roat

Stanford University, Stanford, CA 94305-4060, USA

³Also with IFIC, Instituto de Física Corpuscular, CSIC-Universidad de Valencia, Valencia, Spain

⁴Also with Princeton University

⁵Also with University of California at San Diego

S. Ahmed, M. S. Alam, J. A. Ernst, M. Saleem, F. R. Wappler
State Univ. of New York, Albany, NY 12222, USA

W. Bugg, M. Krishnamurthy, S. M. Spanier
University of Tennessee, Knoxville, TN 37996, USA

R. Eckmann, H. Kim, J. L. Ritchie, R. F. Schwitters
University of Texas at Austin, Austin, TX 78712, USA

J. M. Izen, I. Kitayama, X. C. Lou, S. Ye
University of Texas at Dallas, Richardson, TX 75083, USA

F. Bianchi, M. Bona, F. Gallo, D. Gamba
Università di Torino, Dipartimento di Fisica Sperimentale and INFN, I-10125 Torino, Italy

C. Borean, L. Bosisio, G. Della Ricca, S. Dittongo, S. Grancagnolo, L. Lanceri, P. Poropat,⁶ L. Vitale,
G. Vuagnin

Università di Trieste, Dipartimento di Fisica and INFN, I-34127 Trieste, Italy

R. S. Panvini
Vanderbilt University, Nashville, TN 37235, USA

Sw. Banerjee, C. M. Brown, D. Fortin, P. D. Jackson, R. Kowalewski, J. M. Roney
University of Victoria, Victoria, BC, Canada V8W 3P6

H. R. Band, S. Dasu, M. Datta, A. M. Eichenbaum, J. R. Johnson, P. E. Kutter, H. Li, R. Liu,
F. Di Lodovico, A. Mihalyi, A. K. Mohapatra, Y. Pan, R. Prepost, S. J. Sekula, J. H. von
Wimmersperg-Toeller, J. Wu, S. L. Wu, Z. Yu
University of Wisconsin, Madison, WI 53706, USA

H. Neal
Yale University, New Haven, CT 06511, USA

⁶Deceased

The first observation of color-suppressed B decay modes with hidden strangeness, $s\bar{s}$, was in the decay mode, $B \rightarrow J/\psi\phi K$, by the CLEO collaboration [1] and more recently from the BaBar collaboration [2]. The color suppressed B decay modes are represented at the parton level in Figure 1.

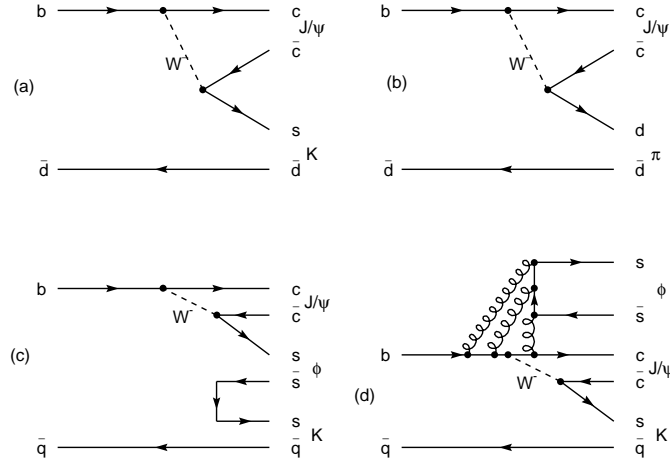


Figure 1: The Feynman diagrams of color-suppressed B decays

Figures 1(a) and (b) show Feynman diagrams for two-body final state color-suppressed B decays into Cabbibo allowed ($J/\psi K$) and Cabbibo suppressed ($J/\psi\pi$) modes. The color suppression is due to the requirement that the color of the quark and anti-quark from the W decay must appropriately be matched with the charm quark and the anti-d quark such that the final state particles are color singlets. Producing a ϕ meson in a three-body final state may be achieved by the addition of $s\bar{s}$ quark-antiquark pairs as shown in Figure 1 (c). It is possible also that a ϕ is formed from three gluon emission as shown in the OZI violating decay in Figure 1(d). Since the η meson is described by the quark-antiquark combination,

$$\eta = \frac{u\bar{u} + d\bar{d} - 2s\bar{s}}{\sqrt{2}}$$

we would also expect B mesons, via the similar diagrams, to decay into states with an η , such as $B \rightarrow J/\psi\eta K$, where the $s\bar{s}$ pairs or two gluons form an η instead of a ϕ . Experimentally, the η is seen in charmless decays at a somewhat anomalously high rate [3], which suggests that gluonic η couplings are large. This may lead to an enhancement in the decay rate of $B \rightarrow J/\psi\eta K$. Since the basic diagrams are the same, we would expect the branching fraction of this mode to be comparable to $\text{BR}(B \rightarrow J/\psi\phi K) = (4.4 \pm 1.4 \pm 0.5) \times 10^{-5}$ [2]. If the rate for non-resonant $B \rightarrow J/\psi\eta K$ is found to be much higher or lower, then some other physics may be indicated.

If the mode $B \rightarrow J/\psi\eta K$ is observed, the neutral mode may be useful for CP violation studies [4], [5] and investigation of quasi-two body decays. The decay, $B \rightarrow \psi(2s)K$, has been observed, and hence the decay $B \rightarrow \psi(2s)K \rightarrow J/\psi\eta K$ should be produced where the $J/\psi\eta$ are in a relative P-wave state with an inferred branching fraction [6] of $B(B^+ \rightarrow \psi(2s)K^+ \rightarrow J/\psi\eta K^+) = (2.1 \pm 0.2) \times 10^{-5}$. If we observe a two body S-wave $J/\psi\eta$ resonance, it would have the quantum

numbers, $J^{PC} = 1^{+-}$, which are those of the unconfirmed h_c . However, since the mass threshold of $J/\psi\eta$ is $3.64 \text{ GeV}/c^2$, which is higher than the lowest lying h_c mass (estimated as the average of the three χ state masses), such an observed resonance could indicate a new particle state. We note in addition that if a $J/\psi\eta$ resonance is found with a mass higher than open charm threshold ($\sim 3.77 \text{ GeV}/c^2$) it is unlikely to be a conventional charmonium state.

The data used in this analysis correspond to a total integrated luminosity of 81.87 fb^{-1} taken on the $\Upsilon(4S)$ resonance producing a sample of 89.96 ± 0.99 million $B\bar{B}$ events ($N_{B\bar{B}}$). The data were collected at the PEP-II asymmetric-energy e^+e^- storage ring with the *BABAR* detector, fully described elsewhere [7]. The *BABAR* detector includes a five-layer silicon vertex tracker (SVT) and a forty-layer drift chamber (DCH) in a 1.5-T solenoidal magnetic field. These devices detect charged particles and measure their momentum and energy loss. Photons and neutral hadrons are detected in a CsI(Tl) crystal electromagnetic calorimeter (EMC). The EMC detects photons with energies as low as 20 MeV and identifies electrons by their energy deposition. An internally reflecting ring-imaging Cherenkov detector (DIRC), composed of quartz bars, measures the charged particle velocity for particle identification. Penetrating muons and neutral hadrons are identified by the steel flux return, which is instrumented with 18-19 layers of resistive plate chambers (IFR).

The preliminary selection criteria in this analysis follow previous *BABAR* analyses [8] and are briefly recalled here. All charged track candidates are required to have at least 12 DCH hits and transverse momentum greater than $100 \text{ MeV}/c$. The track candidates not associated with a K_S^0 decay must also originate near the nominal beam spot. The muon, electron, and kaon candidates must have a polar angle in radians of $0.3 < \theta_\mu < 2.7$, $0.410 < \theta_e < 2.409$, and $0.45 < \theta_K < 2.50$, respectively. In addition, all charged kaon candidates are required to have a laboratory momentum greater than $250 \text{ MeV}/c$. These requirements ensure the selection of tracks in the regions where the acceptance is well understood by the particle identification (PID) systems.

The detailed explanation the PID is given elsewhere [9], [10]. Briefly, photon candidates are identified from energy deposited in contiguous EMC crystals, summed together to form a cluster with total energy greater than 30 MeV and a shower shape consistent with that expected for electromagnetic showers. Electron candidates are required to have a good match between the expected and measured energy loss (dE/dx) in the SVT and DCH, and between the expected and measured Cherenkov angle in the DIRC. The measurements of the ratio of EMC shower energy to track momentum, and the number of EMC crystals associated with the track candidate must be appropriate for an electron. Muons are selected based on the energy deposited in the EMC, the number and distribution of hits in the IFR, the match between the IFR hits and the extrapolation of the track by the DCH into the IFR, and the depth of penetration of the track into the IFR. Charged kaon candidates are selected based on energy loss information from the SVT and DCH and the Cherenkov angle measured by the DIRC.

The intermediate states in the decay modes used in this analysis, $J/\psi(e^+e^-)$, $J/\psi(\mu^+\mu^-)$, and $K_S^0(\pi^+\pi^-)$, are selected within the mass intervals listed in Table 1. The di-electron mass interval is larger than the di-muon to account for Bremstrahlung in the detector. The K_S^0 decay length is required to be greater than 0.1 cm.

The remaining four selection criteria are the η mass, the π^0 veto, the photon helicity angle [8] from the η decay and the thrust angle. In the following we describe each of these criteria and the process used to determine their final cut values.

The η candidates are required to have $\gamma\gamma$ mass within the range listed in Table 1. If either of the photons associated with an η candidate, in combination with any other photon in the event, forms a $\gamma\gamma$ mass near the nominal π^0 mass, the η candidate is vetoed as a π^0 background. The

π^0 veto selection was adjusted by limiting the mass difference between all possible $\gamma\gamma$ masses and the nominal π^0 mass as shown Table 1. The η candidate is rejected if $|\cos\theta_\gamma^\eta|$ is near 1, where θ_γ^η is the photon helicity angle in the η rest frame. This rejects combinatoric background due to random pairs of photons that typically have a photon helicity angle distribution that peaks at 0 or 180 degrees.

An additional requirement is applied to separate two-jet continuum events from the more spherical B meson decays. The angle θ_T between the thrust [8] direction of the B meson candidate and the thrust direction of the remaining tracks in the event is calculated. We reject events when $|\cos\theta_T|$ is near 1, since the distribution in $\cos\theta_T$ is flat for $B\bar{B}$ events, while for background continuum events the distribution is peaked at $\cos\theta_T = \pm 1$.

Estimation of the signal and the background use two kinematic variables: the energy difference ΔE between the energy of the B candidate and the beam energy E_b^* in the $\Upsilon(4S)$ rest frame; and the energy-substituted mass $m_{ES} = \sqrt{(E_b^*)^2 - (P_B^*)^2}$, where P_B^* is the reconstructed momentum of the B candidate in the $\Upsilon(4S)$ frame. Typically these two variables in a two-dimensional plot for the B meson signal will appear as a weakly correlated two-dimensional Gaussian distribution, whereas the background is roughly uniformly distributed. The ΔE and m_{ES} resolutions are mode dependent. A signal region for each mode, B^+ and B^0 , is defined as a rectangular region in the ΔE versus m_{ES} plane with $|m_{ES} - m_B| < 7.5 \text{ MeV}/c^2$, where m_B is the mass of B meson and $|\Delta E| < 40 \text{ MeV}$. Before the data were analyzed, these four final selection criteria were optimized using a Monte Carlo (MC) simulation of the signal and the known backgrounds. Motivated by the $B \rightarrow J/\psi\phi K$ measurement, the *ab initio* value of the branching fraction for $B \rightarrow J/\psi\eta K$ used in the signal MC was 5×10^{-5} . The number of reconstructed MC signal events (n_s^{mc}) and the number of reconstructed MC background events (n_b^{mc}) in the signal box were obtained using the same criteria to estimate the signal significance ratio, $n_s^{mc}/\sqrt{n_s^{mc} + n_b^{mc}}$. This ratio was maximized by varying these four selection criteria. The resulting criteria were fixed and are listed in Table 2. The resulting ΔE and m_{ES} distributions for data are shown in Figs. 2 and 3. The number of data events (n_0) observed in the signal box region for each mode, B^+ and B^0 , is listed in Table 3.

The m_{ES} distribution background shape is determined by fitting the line shape of an ARGUS function [8] for each mode to the m_{ES} distributions formed from the ΔE sideband region of the on-peak data of $0.1 < |\Delta E| < 0.14$ for the B^+ mode and $0.08 < |\Delta E| < 0.28$ for the B^0 mode. To determine the number of signal events, we fit the data m_{ES} distribution to a model (see Figs. 2(c) and 3(c)) that is the sum of this ARGUS function whose normalization is allowed to vary, and a signal Gaussian, whose width is fixed to the MC value but whose mean and normalization are allowed to vary. The integral of this resulting ARGUS function over the signal box region yields the number of background events (n_b) and its uncertainty (σ_b). Similar m_{ES} background shapes were found by using a $\gamma\gamma$ mass sideband outside the nominal η mass. Occasionally backgrounds with an inclusive J/ψ decay will lead to a peaking background near or at the B mass in the m_{ES} distribution. Background shapes consisting of a sum of the ARGUS function and a broad Gaussian were attempted, however its contribution was found to be small and was dropped from the final background fit. The final values of n_b and σ_b are listed in Table 3.

We find evidence for signals in the $J/\psi\eta K^+$ and $J/\psi\eta K_S^0$ modes as seen in Figs. 2 and 3. To determine the branching fraction for these modes the number of signal events (n_s) is given by a simple subtraction of the estimated number of background events from the events in the signal box region, $n_s = n_0 - n_b$. The efficiencies (ϵ) for each mode, listed in Table 3, are determined by MC simulation with three-body phase space and unpolarized J/ψ decays. The calculation of the

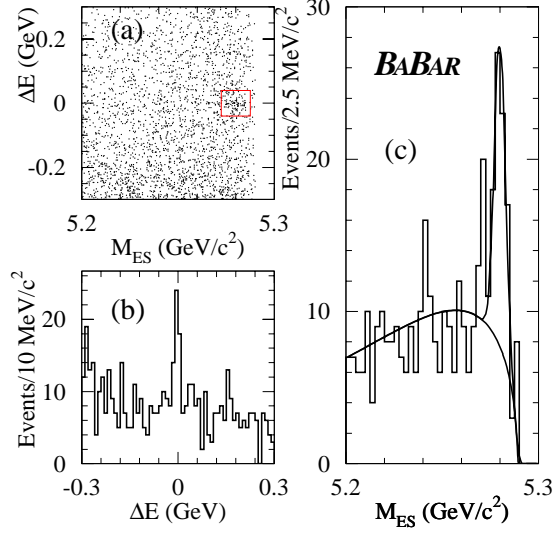


Figure 2: The ΔE and m_{ES} distributions for $B^+ \rightarrow J/\psi\eta K^+$. The ΔE vs. m_{ES} event distribution is shown in (a) with a small rectangle corresponding to the signal region selection defined in the text. The ΔE projection within a m_{ES} signal region selection is shown in (b). The m_{ES} projection within a ΔE signal region selection is shown in (c). The solid line in (c) is the fit described in the text.

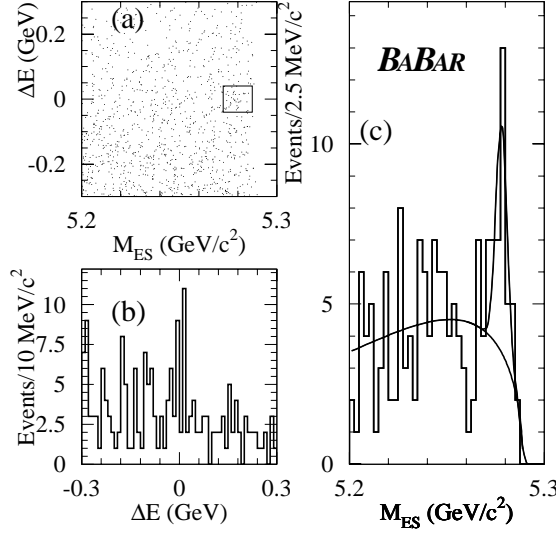


Figure 3: The ΔE and m_{ES} distributions for $B^0 \rightarrow J/\psi\eta K_S^0$. The descriptions of Figs. 3(a), (b) and (c) follow those of Figs. 2(a), (b) and (c), respectively.

branching fraction (BF) is

$$BF = \frac{n_s}{N_{B\bar{B}} \times \epsilon \times f}$$

where ϵ is the efficiency for the mode and f is the product of secondary branching fractions for the J/ψ , η , and K_S^0 . The results are given in the last column of Table 3 where the first and second BF uncertainties are the statistical and systematic, respectively. The statistical uncertainty is derived from the error on n_s which is $\sqrt{n_0 + \sigma_b^2}$.

In Table 4, we list the contribution to the systematic uncertainty from the error on each of the following quantities: $N_{B\bar{B}}$; secondary branching fractions [6]; MC statistics; PID, tracking, and photon detection efficiencies; π^0 veto; η mass range; background parameterization; and model dependence. The PID, tracking, and photon detection efficiency uncertainties are based on the study of data control samples [11]. The error in the π^0 veto efficiency was studied by measuring the inclusive η rate in both data and MC. After varying the π^0 veto mass cut, the change in the number of inclusive η 's was determined in data and MC to measure the deviation between the data and the simulation and to estimate the resulting systematic uncertainty. The uncertainty in the η mass range was determined by comparing the measured η mass resolution in inclusive η decays to the η mass resolution from the signal MC. The background parameterization uncertainty was estimated by changing the ARGUS shape parameter by ± 1 standard deviation, refitting the m_{ES} data distribution and recalculating the number of signal events. Additional systematic uncertainties due to the decay model dependence are estimated for the modes $J/\psi\eta K^+$ and $J/\psi\eta K_S^0$. MC simulations are used to determine how much the efficiency depends on assumptions about intermediate resonances and angular distributions. Five samples were studied. One sample is generated with 100% transversely polarized J/ψ and another with 100% longitudinally polarized J/ψ . The other three samples had large $J/\psi\eta$ mass, large ηK mass or small $J/\psi K$ mass. The resulting relative change in efficiency is entered as a fractional systematic uncertainty in Table 4. The total systematic uncertainty for each mode combines all these separate errors in quadrature, is listed the last column in Table 4. and is used to determine the BF systematic uncertainties listed in Table 3.

The probability for a null hypothesis (P-value) is defined as the Poisson probability that the estimated number of background events fluctuates to observed number of events n_0 or greater. In Table 3 we provide P-values calculated using the central value of the background estimate n_b and the value increased by 1 standard deviation, $n_b + \sigma_b$, to provide an estimate of probability including the background systematic uncertainty.

We determine also the 90% confidence level upper limit on the branching fraction using n_0 , n_b , and σ_b , in the signal region, and the total systematic uncertainty σ_T . Assuming the two uncertainties (σ_b, σ_T) are uncorrelated and Gaussian, the Bayesian upper limit on the number of events ($N_{90\%}$) is obtained by folding the Poisson distribution with two normal distributions describing these two uncertainties and integrating the resulting function to the 90% confidence level (C.L.). This assumes that the *a priori* branching fraction distributions are uniform. The results are listed in Table 3.

Our preliminary branching fraction is comparable to $B \rightarrow J/\psi\phi K$ and is consistent with simple expectations from color-suppressed decay diagrams. The ratio of the charged ($J/\psi\eta K^\pm$) to neutral ($J/\psi\eta K_S^0$) branching fractions is expected to be two which is not inconsistent with our results. Although the current statistics are too small, a larger data set of the neutral mode could be useful for a test of CP violation and both charged and neutral modes may enable a search for resonances in the two body intermediate states.

In summary, we find evidence for the decay $B \rightarrow J/\psi\eta K$ in two modes with preliminary branching fractions of, $\mathcal{B}(B^+ \rightarrow J/\psi\eta K^+) = (10.8 \pm 2.3 \pm 2.4) \times 10^{-5}$ and $\mathcal{B}(B^0 \rightarrow J/\psi\eta K_S^0) = (8.4 \pm 2.6 \pm 2.7) \times 10^{-5}$.

We are grateful for the excellent luminosity and machine conditions provided by our PEP-II

colleagues, and for the substantial dedicated effort from the computing organizations that support *BABAR*. The collaborating institutions wish to thank SLAC for its support and kind hospitality. This work is supported by DOE and NSF (USA), NSERC (Canada), IHEP (China), CEA and CNRS-IN2P3 (France), BMBF and DFG (Germany), INFN (Italy), FOM (The Netherlands), NFR (Norway), MIST (Russia), and PPARC (United Kingdom). Individuals have received support from the A. P. Sloan Foundation, Research Corporation, and Alexander von Humboldt Foundation.

References

- [1] CLEO Collaboration, A. Anastassov *et al.*, Phys. Rev. Lett. **84**, 1393 (2000).
- [2] *BABAR* Collaboration, B. Aubert *et al.*, SLAC-PUB-9262, submitted to Phys. Rev. Lett.
- [3] CLEO publication, S.J. Richichi *et al.*, Phys. Rev. Lett. **85**, 520 (2000).
- [4] M. Kobayashi and T. Maskawa, Prog. Th. Phys. **49**, 652 (1973).
- [5] *BABAR* Collaboration, B. Aubert *et al.*, Phys. Rev. Lett. **86**, 2515 (2001), B. Aubert *et al.*, Phys. Rev. Lett. **87**, 91801 (2001), B. Aubert *et al.*, Phys. Rev. **D66**, 32003 (2002); *Belle* Collaboration, K. Abe *et al.*, Phys. Rev. Lett. **86**, 2509 (2001), K. Abe *et al.*, Phys. Rev. Lett. **87**, 91802 (2001), K. Abe *et al.*, Phys. Rev. **D66**, 71102 (2002);
- [6] Particle Data Group, K. Hagiwara *et al.*, Phys. Rev. **D66**, 010001 (2002).
- [7] *BABAR* Collaboration, B. Aubert *et al.*, Nucl. Instr. and Methods **A479**, 1 (2002).
- [8] *BABAR* Collaboration, B. Aubert *et al.*, Phys. Rev. **D65**, 32001 (2002). This publication forms a basic reference of our analysis. The helicity angles and thrust variable are described in section VIIC.1, the ARGUS function and beam energy substituted mass in section VIIC, and the particle identification and tracking criteria for the photons, electrons and muons in sections IIC and IID.
- [9] The particle identification selection is taken from ref. [8]. The photon candidates selection is the same as that in ref. [8]. The electron candidates are required to satisfy the “Tight” selections and the muon candidates use the “Loose” selections, as specified in ref. [8].
- [10] *BABAR* Collaboration, B. Aubert *et al.*, Phys. Rev. **D66**, 32003, (2002). The charged kaon candidate used a selection slightly more stringent than those described in this reference.
- [11] The estimate of the uncertainty on the PID, tracking and photon detection efficiency using control samples from data is described in section XI of ref. [8].

TABLES

Table 1: Mass regions for selection of intermediate particles.

Mode	Mass Range (GeV/c ²)			
$J/\psi \rightarrow e^+e^-$	2.95	<	$M(e^+e^-)$	< 3.14
$J/\psi \rightarrow \mu^+\mu^-$	3.06	<	$M(\mu^+\mu^-)$	< 3.14
$K_S^0 \rightarrow \pi^+\pi^-$	0.489	<	$M(\pi^+\pi^-)$	< 0.507
$\eta \rightarrow \gamma\gamma$	0.525	<	$M(\gamma\gamma)$	< 0.571

Table 2: Final selection criteria for the $B^\pm \rightarrow J/\psi\eta(\gamma\gamma)K^\pm$ and $B^0 \rightarrow J/\psi\eta(\gamma\gamma)K_S^0$ modes.

Variable	$J/\psi\eta K^+$	$J/\psi\eta K_S^0$
$ M_\eta - 0.547 \leq$	0.023 GeV/c ²	0.023 GeV/c ²
π^0 veto if $ M(\gamma_\eta + \gamma_{other}) - 0.135 \leq$	0.017 GeV/c ²	0.010 GeV/c ²
Helicity: $ \cos(\theta_\gamma^\eta) \leq$	0.93	0.81
Thrust: $ \cos(\theta_T) \leq$	0.8	0.9

Table 3: Branching fractions and 90% C.L. upper limits.

Mode	ϵ	n_0	$n_b \pm \sigma_b$	$N_{90\%}$	90% C.L.U.L. (10 ⁻⁵)	P-value range	Branching Fraction (10 ⁻⁵)
$J/\psi\eta K^+$	10.75%	99	50.3 ± 3.0	70.0	<15.5	$(0.09 - 1.42) \times 10^{-8}$	$10.81 \pm 2.31 \pm 2.37$
$J/\psi\eta K_S^0$	8.53%	39	18.5 ± 1.7	34.5	<14.1	$(.23 - 1.3) \times 10^{-4}$	$8.35 \pm 2.64 \pm 2.67$

Table 4: Systematic uncertainty summary on the branching fractions. All are fractional uncertainties in percent.

Mode	$N_{B\bar{B}}$	Secondary Branching Fraction	M.C. Stat.	PID, tracking, γ Det.	π^0 veto	η mass cut	Bkgd. Param.	Model	Total
$J/\psi\eta K^+$	1.1	2.48	1.77	8.2	8.1	3.40	16.7	5.1	22.0
$J/\psi\eta K_S^0$	1.1	2.52	2.17	8.3	8.3	3.14	27.0	9.5	32.0